

Supporting Information for

Pb-activated Amine-assisted Photocatalytic Hydrogen Evolution Reaction on Organic-Inorganic Perovskites

Lu Wang^{*,†,‡}, Hai Xiao[‡], Tao Cheng[‡], Youyong Li^{*,†}, William A. Goddard III^{*,‡}

[†]Institute of Functional Nano & Soft Materials (FUNSOM), Jiangsu Key Laboratory for Carbon-Based Functional Materials & Devices, Soochow University, Suzhou, Jiangsu 215123, China

[‡]Materials and Process Simulation Center (MSC) and Joint Center for Artificial Photosynthesis (JCAP), California Institute of Technology, Pasadena, California 91125, United States

Computational Methods:

We used the PBE functional¹ of density functional theory (DFT) including the D3 van der Waals correction to account for London dispersion interactions.² All calculations were performed in the VASP package³⁻⁵ using the projector augmented wave (PAW) method to account for core-valence interactions.⁶ The kinetic energy cutoff for plane wave expansions was set to 350 eV, and reciprocal space was sampled using the Γ -point scheme. We applied Gaussian smearing using a small width of 0.05 eV. Transition state (TS) searches were conducted using the climbing image nudged elastic band (CI-NEB) method to generate the reaction path and the transition state structure.⁷ All initial state (IS) and final state (FS) geometries were converged to within 5×10^{-2} eV/Å for maximal components of forces, and the forces on TS structures were converged to 0.1 eV/Å.

Details of our structural model:

In our structural model, we consider the 2×2 supercell of the (010) surface of orthorhombic MAPbI₃ perovskite (lattice parameters of $17.887 \text{ \AA} \times 17.114 \text{ \AA}$), which was confirmed to be a stable surface for the orthorhombic structure.⁸ To describe the electrode-electrolyte interface (EEI), we include three layers of explicit water (64 H₂O, 0.78 nm thick) on the MAPbI₃ surface slab (monolayer). The double-layer model is compared in Table S1 of Supporting Information, which indicates monolayer model is adequate to describe the HER reaction on the MAPbI₃ surface. Experimentally, the H₂ is generated in HI containing aqueous solution, so we replace three H₂O molecules with HI molecules to simulate the acidic environment (pH=-0.48). With structural relaxation, the three HI molecules dissociate to form three I⁻ ions plus three H₃O⁺ molecules in the solution. To describe the photoexcited state, we added two potassium atoms to populate the

conduction band of the perovskite. The whole system is fully relaxed, except that the bottom organic iodide layer is fixed.

We have compared the reaction energies and activation barriers between single-layer model (only the bottom MA iodide layer is fixed) and double-layer model (the top layer is fully relaxed and the second layer is fixed) of MAPbI₃. The results are shown in the below Table S1. Indeed, the results are very close. Therefore, we consider that the thickness of our structural model has little effect on the surface HER reaction, and single-layer structural model seems to be adequate to describe the HER reaction on the MAPbI₃ surface.

Table S1. Energy difference, rate-determining barrier and H-Pb bond length in the intermediate structure calculated on single-layer model and double layer model.

Reaction energy	Initial structure	Intermediate structure	H-Pb bond length in intermediate structure	Final structure	Rate-determining barrier
Single layer	0	-1.349 eV	1.970 Å	-3.645 eV	1.080 eV
Double layer	0	-1.418 eV	1.964 Å	-3.649 eV	1.064 eV

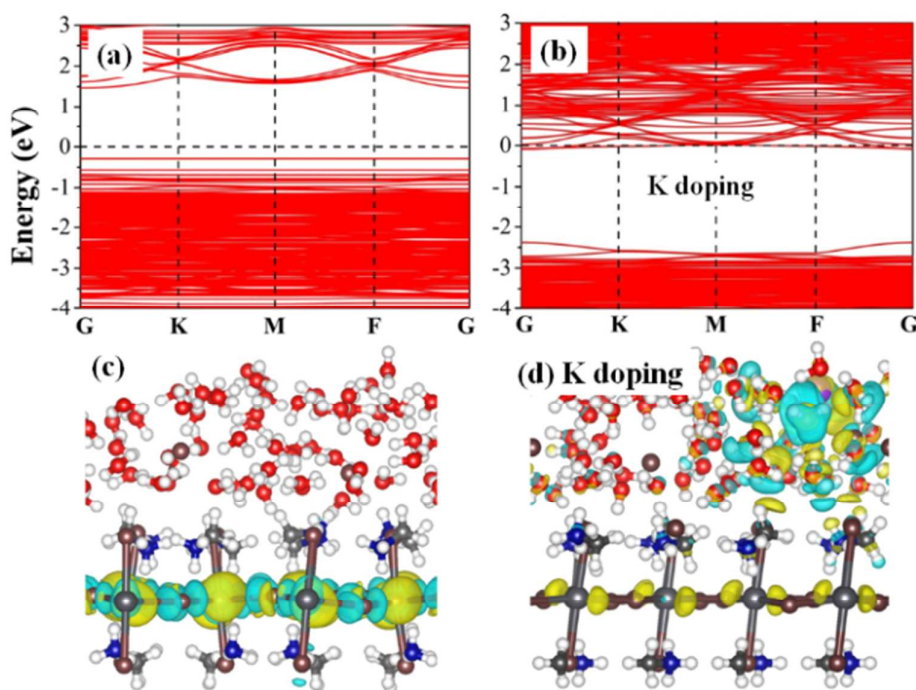


Fig. S1. (a) Band structure of MAPbI₃ in explicit water solvent (at pH=-0.48); (b) band structure of MAPbI₃ with potassium atoms added to simulate the photoexcited state; (c) the optimum structure of MAPbI₃ for the triplet excited state (to mimic the exciton); (d) the charge difference between the system with and without potassium atom doping (singlet state). The yellow and cyan colors indicate the distributions of electrons and holes, respectively. The Fermi level is set to zero.

Our structural model explicitly includes the EEI between the water solution and MAPbI₃ surface, allowing surface reconstruction. The MA⁺ molecules on the surface exhibit two orientations. Some MA⁺ cations have the -NH₃ pointed upward forming hydrogen bonds (HB) with the first layer of H₂O, while the others have the -NH₃ pointed downward to form HB to the second layer I anions, similar to the surface structure in a vacuum. The band structure for the MAPbI₃ surface in water solution is shown in Fig. 1(a). We find a band gap of 1.76 eV in solvent (2.30 eV in vacuum). For the excited state under visible light irradiation, the electrons and holes separate with the electrons associated with Pb atoms while the holes are associated with I atoms, which we simulate here by calculating the triplet state, Fig. 1(c). After doping with two potassium atoms to mimic the photoexcited state, the semiconductor has two electrons in the conduction band, defining the Fermi level (Fig. 1(b)). Here the conduction band minimum is dominated by the 6*p* character of lead atoms, so the extra two electrons are located on lead atoms, which is also confirmed by the charge difference analysis in Fig. 1(d). Such delocalized electrons over Pb atoms are consistent with the previous studies.^{9,10}

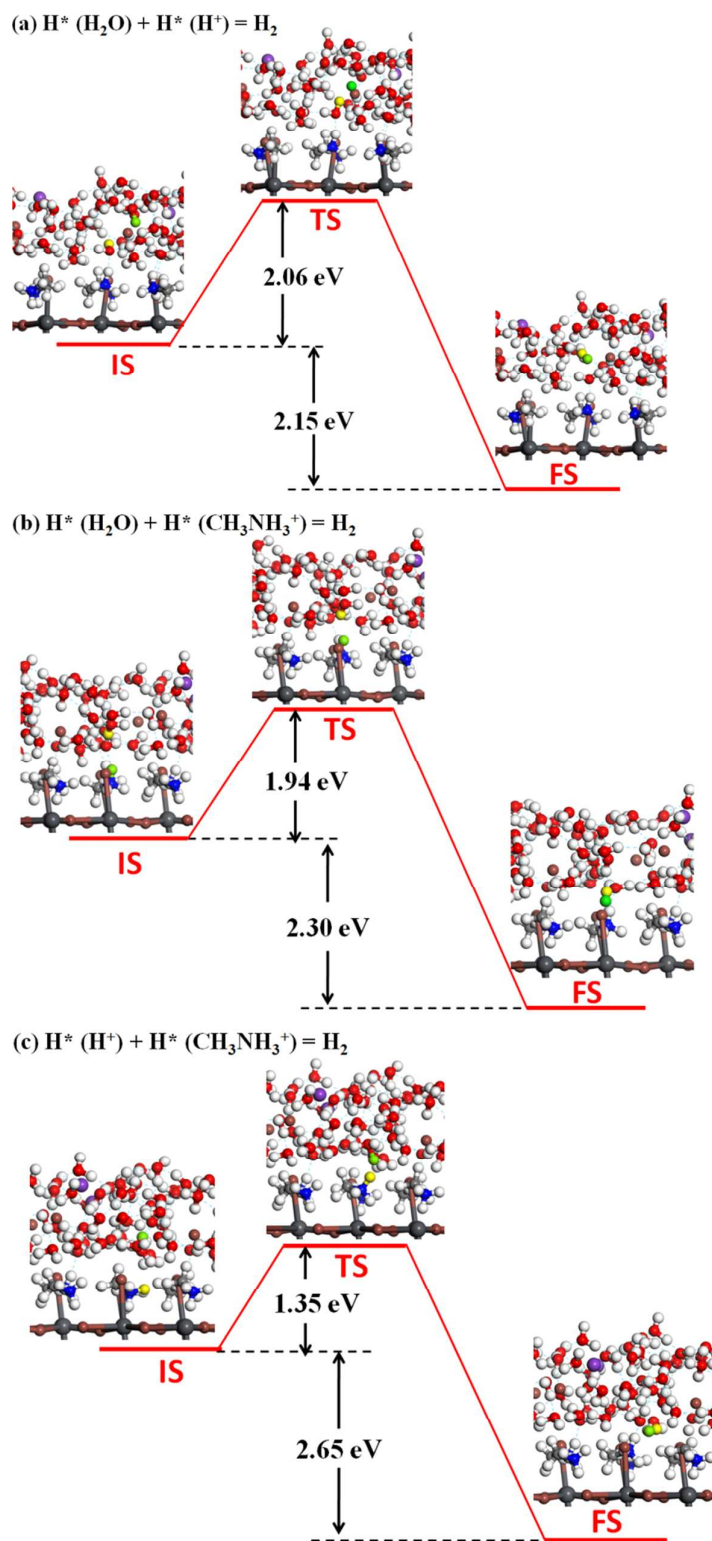


Fig. S2. The initial structures, transition states and final structures for the three possible pathways of H_2 generation on MAPbI_3 surface together with the activation barriers and reaction energies. The two H of H_2 product are highlighted by yellow and green color.

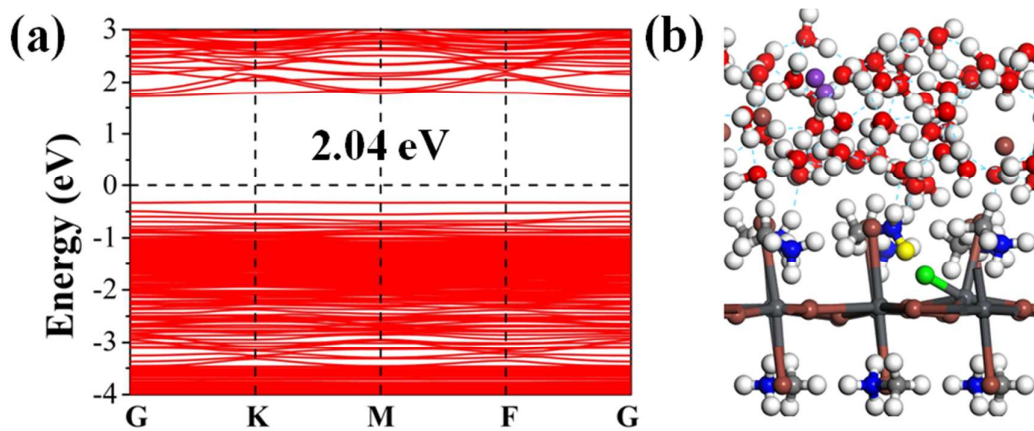


Fig. S3. (a) Band structures and (b) geometries of the intermediate state of lead hydride.

Results in the dark condition:

We also calculated the same reaction mechanism for H_2 generation for the dark reaction. To do this, we removed the two potassium atoms whose electrons had gone to the conduction band. We then optimized the initial structure, intermediate state and final structure, which are shown in Fig. S3 of the Supporting Information. Here we note that, the structure of the intermediate state has the H of MA^+ forming an H-I bond to the I atom in the lead iodide layer, not the lead hydride that we find stable with photoexcitation. This is because no extra electron is located at the lead atom, so the H from MA^+ prefers to bond to the negative charged I. The activation barrier for this reaction is calculated to be 2.61 eV. Then, the second H in the recovered MA^+ moves to the H in H-I to form the H_2 molecule. This second reaction has an activation barrier of 2.25 eV. The energies for these two reactions are endothermic by a total energy of 1.92 eV. This large energy barrier for the dark condition is close to that of 2.96 eV for electrolysis of water under standard conditions. This is consistent with the recent experiment observations.¹¹

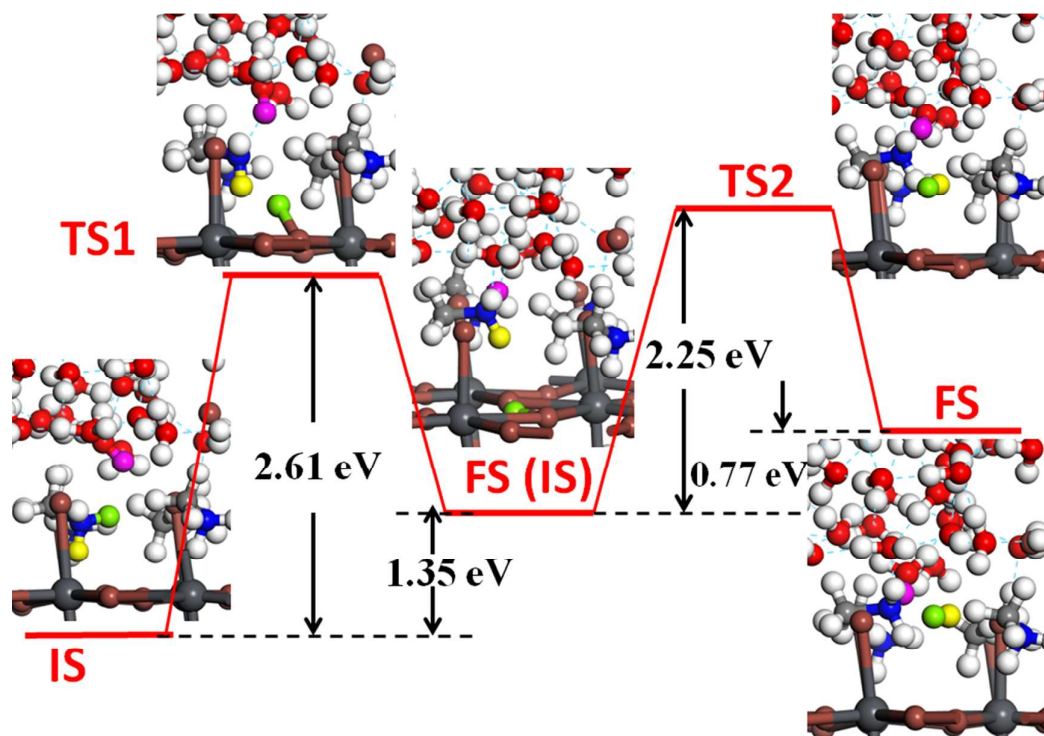


Fig. S4. The reaction pathway for the H_2 generation in the dark condition, and the activation barriers and reaction energies are also shown.

References:

- (1) Perdew, J. P.; Burke, K.; Ernzerhof, M. *Phys.Rev. Lett.* **1996**, *77*, 3865.
- (2) Grimme, S.; Antony, J.; Ehrlich, S.; Krieg, H. *J. Chem. Phys.* **2010**, *132*, 154104.
- (3) Kresse, G.; Hafner, J. *Phys. Rev. B* **1993**, *47*, 558.
- (4) Kresse, G.; Furthmüller, J. *Phys.Rev. B* **1996**, *54*, 11169.
- (5) Kresse, G.; Furthmüller, J. *Comput. Mater. Sci.* **1996**, *6*, 15.
- (6) Kresse, G.; Joubert, D. *Phys. Rev. B* **1999**, *59*, 1758.
- (7) Henkelman, G.; Uberuaga, B. P.; Jónsson, H. *J. Chem. Phys.* **2000**, *113*, 9901.
- (8) Ohmann, R.; Ono, L. K.; Kim, H.-S.; Lin, H.; Lee, M. V.; Li, Y.; Park, N.-G.; Qi, Y. *J. Am. Chem. Soc.* **2015**, *137*, 16049.
- (9) Santomauro, F. G.; Grilj, J.; Mewes, L.; Nedelcu, G.; Yakunin, S.; Rossi, T.; Capano, G.; Haddad, A. A.; Budarz, J.; Kinschel, D.; Ferreira, D. S.; Rossi, G.; Tovar, M. G.; Grolimund, D.; Samson, V.; Nachtegaal, M.; Smolentsev, G.; Kovalenko, M. V.; Chergui, M. *Struct. Dyn.* **2017**, *4*, 044002.
- (10) Zhang, L.; Sit, P. H. L. *J. Mater. Chem. A* **2017**, *5*, 23976.
- (11) Park, S.; Chang, W. J.; Lee, C. W.; Park, S.; Ahn, H.-Y.; Nam, K. T. *Nat. Energy* **2016**, *2*, 16185.